Wojciech Dziembowski, Warsaw Univ. Obs.

Nonradial oscillations in giants and supergiants – an update

Nov 08, 2011

KITP Asteroseismo

Red giant oscillations from **OGLE**, **CoRoT** and ***KEPLER*** data

Varibility in RGB and AGB stars

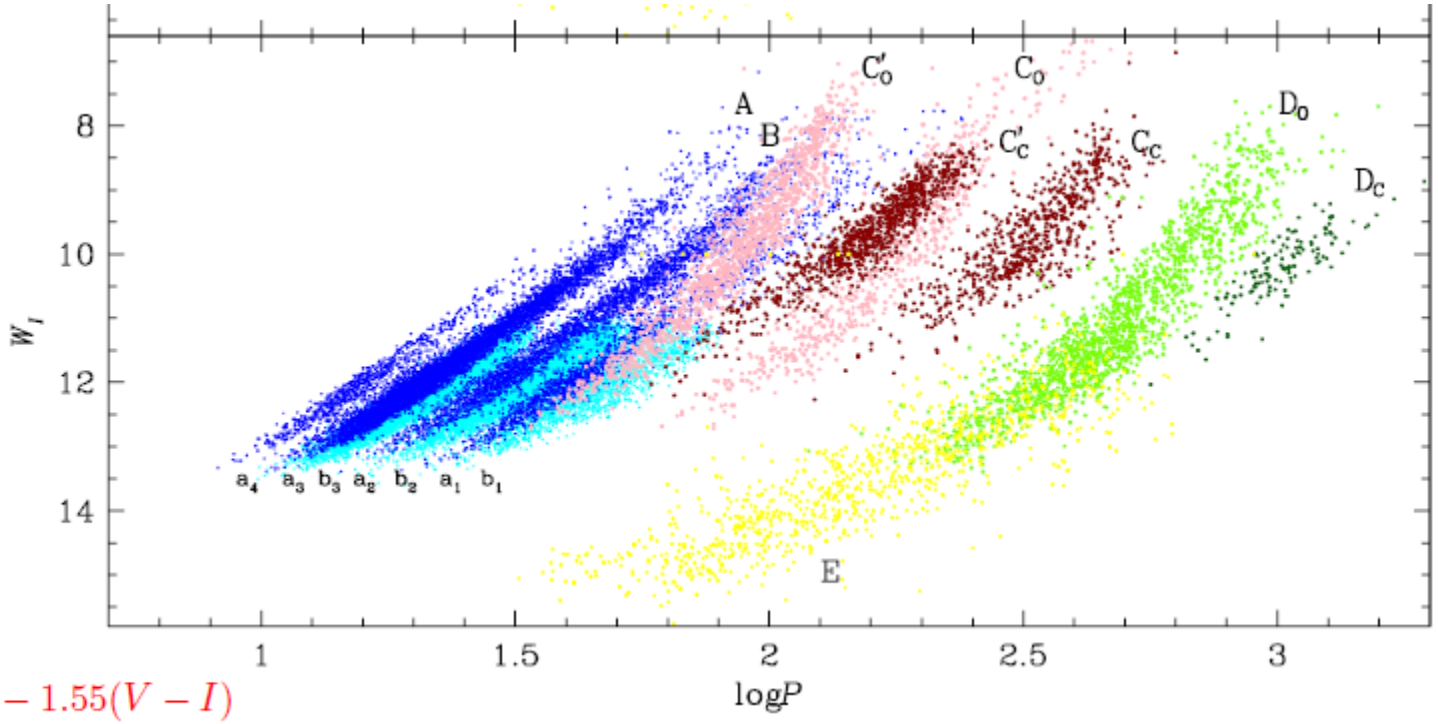

$W_I = I - 1.55(V - I)$

The many PL relations from the OGLE project (Soszyński et al., 2007)

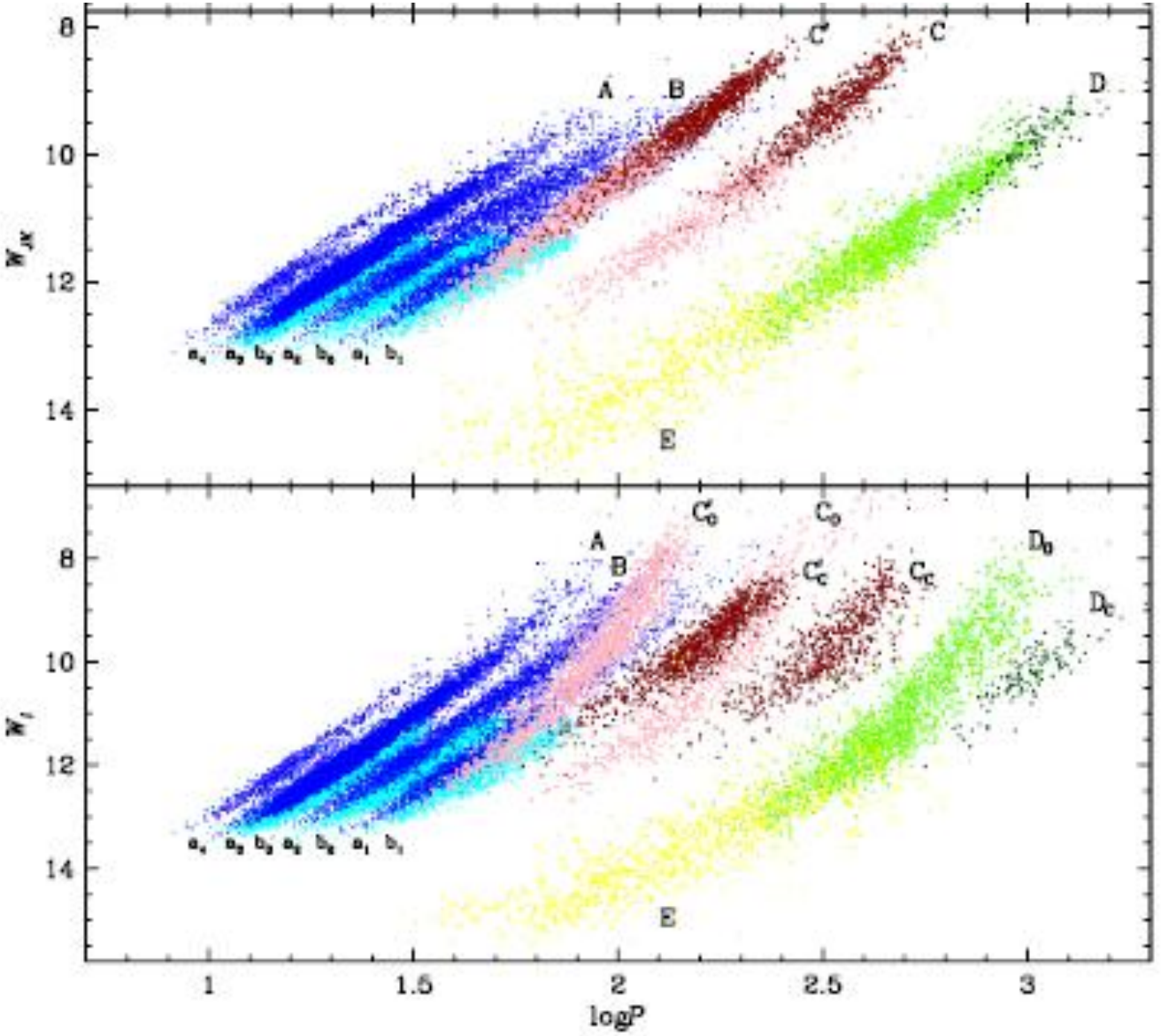

Fig. 1. Period–luminosity diagrams of variable red giants in the LMC. OSARG variables are shown as blue points (RGB as light blue, AGB as dark blue). Miras and SRVs are marked with pink (O-rich) and red (C-rich) points. Light and dark green points refer to O-rich and C-rich LSP variables, respectively. Yellow points indicate ellipsoidal red giants.

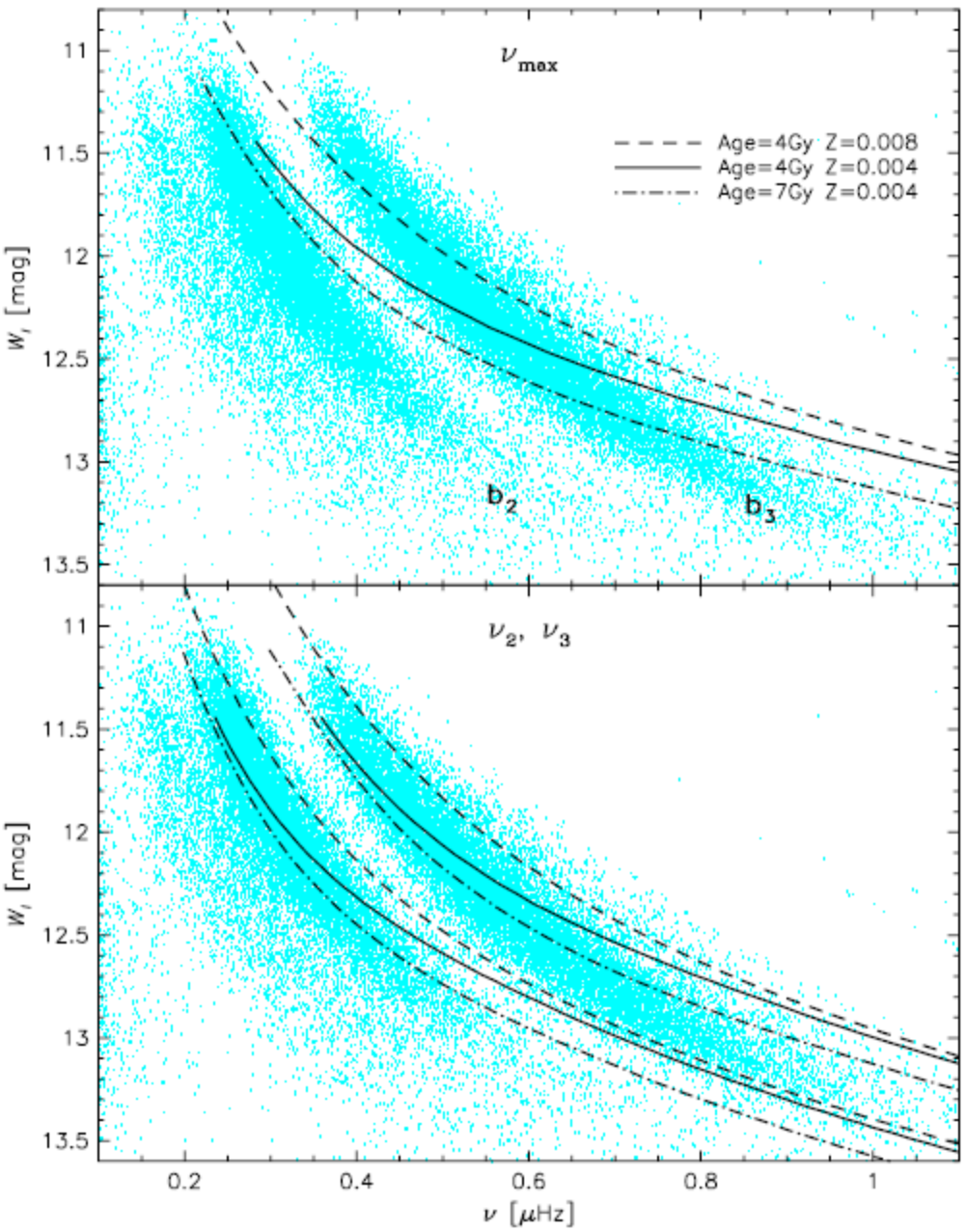

B – type *OSARG*
= solar type oscillations in extreme red giants?
(Soszyński et sl. 2007, Dz. & Soszyński 2010)

$$W_I = 12\text{mag} \rightarrow \log \frac{L}{L_\odot} \approx 3.2 \times 10^3$$

$$\nu_{\max} = \frac{L_\odot}{L} \frac{M}{M_\odot} \left(\frac{T}{T_\odot} \right)^{3.5} \times 3050 \mu\text{Hz}$$

$$A_I = \left(\frac{L}{L_\odot} \frac{M_\odot}{M} \right)^s \left(\frac{T_\odot}{T} \right)^2 \times 0.0035\text{mmag}.$$

$$s \approx 0.93$$

Soszyński & al., 2007

Log *L* @ *M*_0=1

Global picture of red giant oscillations from CoRot data

RC: log *L* =1.68
M=0.89

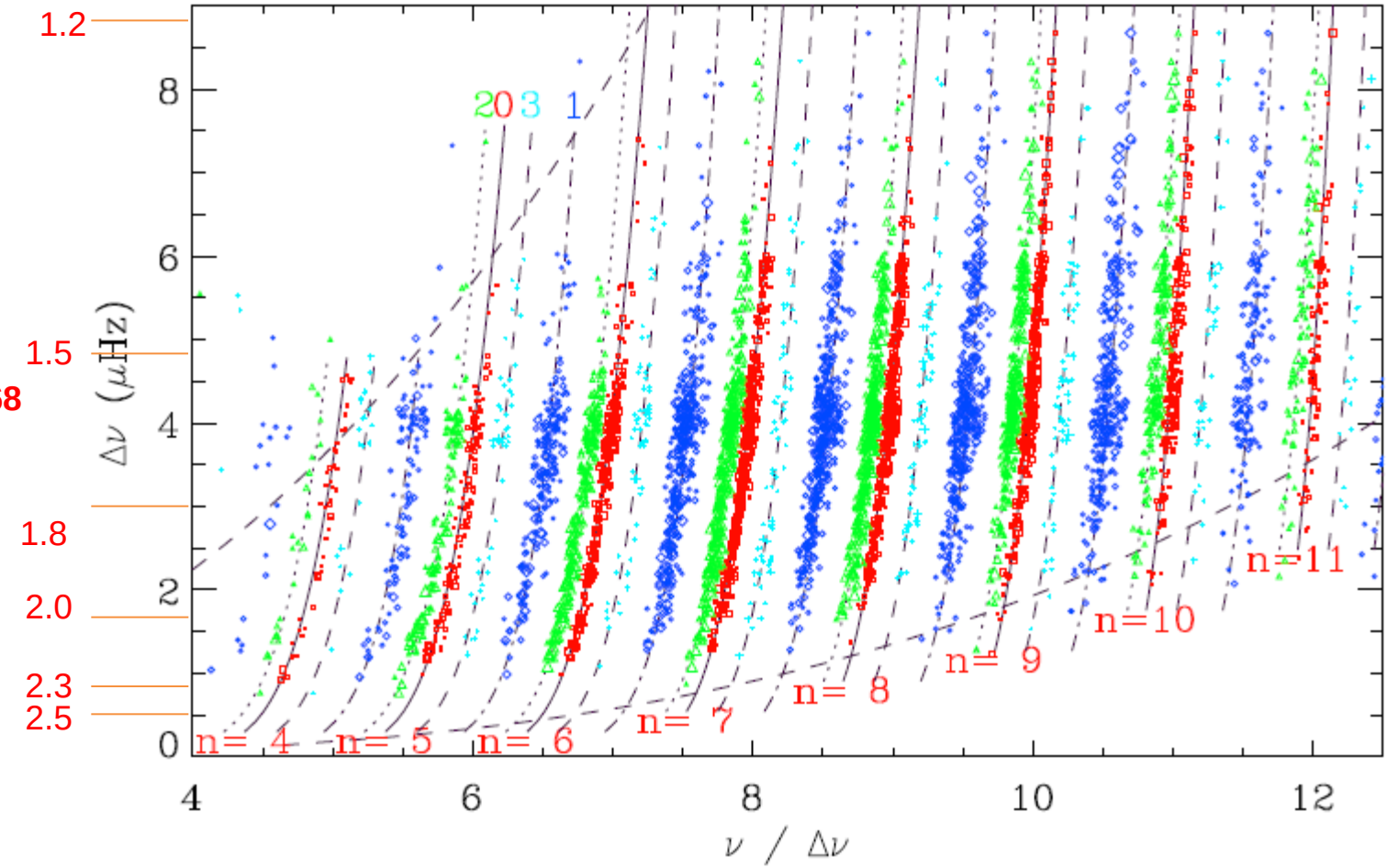

$$\nu_{\max} = \frac{L_\odot}{L}\frac{M}{M_\odot}\left(\frac{T}{T_\odot}\right)^{3.5} \times 3050\mu\mathrm{Hz}$$

Mosser et al.,2010

Mixed modes in red giants from *Kepler data*

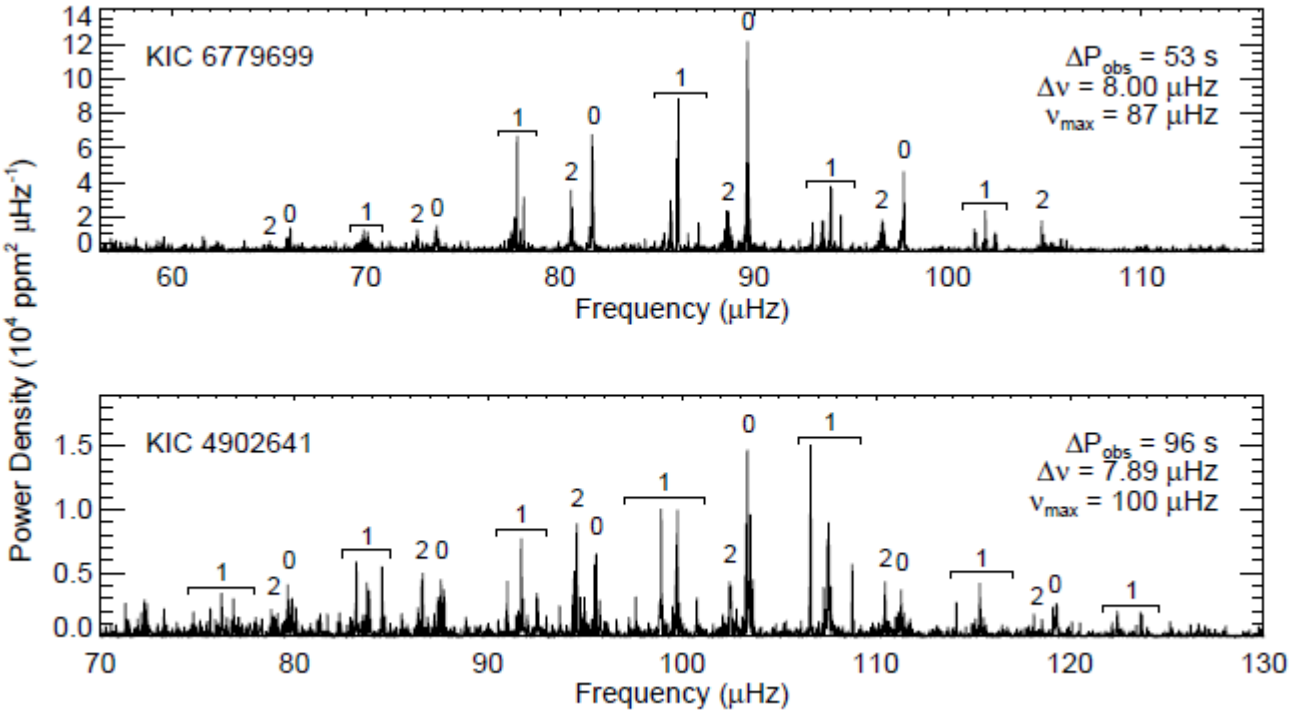

Lower RGB object
small degenrate He core

red clump
He –burning phase

$$\Delta P \sim \left(\int_{r_0}^{r_b} \mathcal{N} \frac{\mathrm{dr}}{\mathrm{r}} \right)^{-1} \sim \frac{\bar{\rho}}{\bar{\rho}_{\mathrm{core}}}$$

Bedding et al. (2011)

Mixed modes in red giants from *KEPLER* data

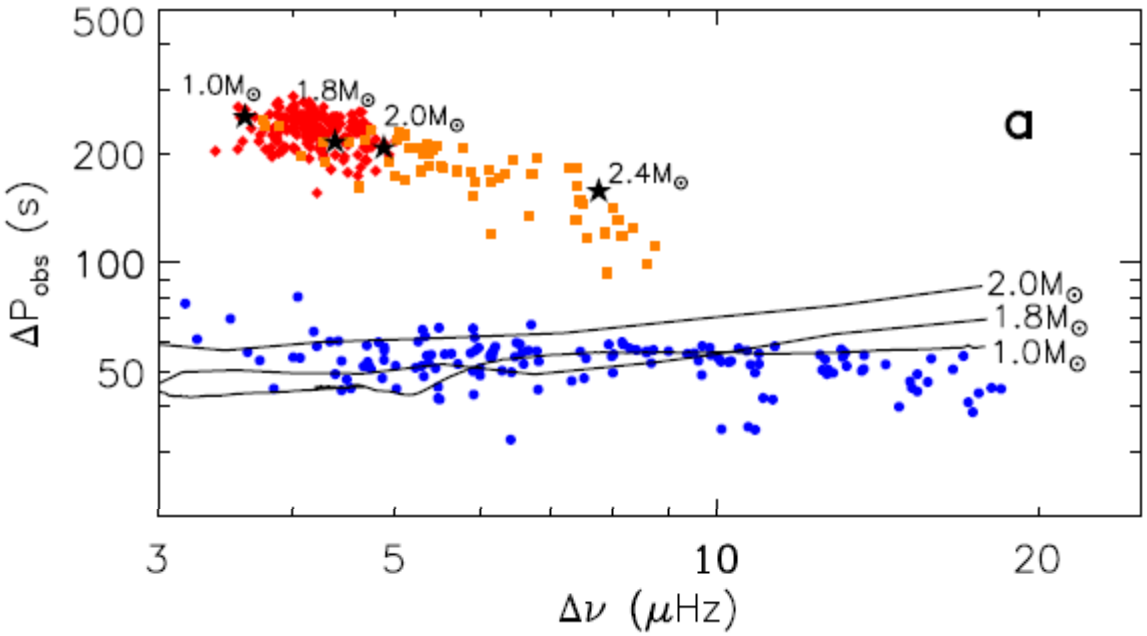

Bedding et al. (2011)

Unstable nonradial modes in classical pulsators

(Osaki 1977, Dziembowski1977)

Eigenfunctions in radiative interior

$$N \gg \omega \qquad \mathcal{L}_\ell \gg \omega$$

$$\xi_r \approx \frac{C_+ \mathrm{e}^{\mathrm{i}\Psi} + C_- \mathrm{e}^{-\mathrm{i}\Psi}}{r^2\sqrt{|k_r|\rho}} Y_\ell^m \mathrm{e}^{-\mathrm{i}\omega t} \qquad \Psi = \Psi_0 + \int_{r_0} k_r \mathrm{d}r \qquad \text{(complex)}$$

$$k_r \simeq \frac{\sqrt{\ell(\ell+1)}}{\omega_R}\frac{N}{r}[1 - \mathrm{i}(\mathcal{D} + \frac{\omega_I}{\omega_R})] \qquad \mathcal{D} = \frac{\ell(\ell+1)}{8\pi\omega^3}\frac{gL_\mathrm{r}}{r^4 p}\frac{\nabla_\mathrm{ad}}{\nabla}(\nabla_\mathrm{ad} - \nabla)$$

From standing to running waves

$$|\Im(\Psi)| \gg 1 \qquad \Im(k_r) < 0 \qquad \longrightarrow \qquad C_- = 0$$

Trapped modes may be unstable in spite of the wave losses

RR Lyrae star models

l=10 modes calculated
With the running wave
boundary condition

$$n_g \sim 10^2\sqrt{\ell}$$

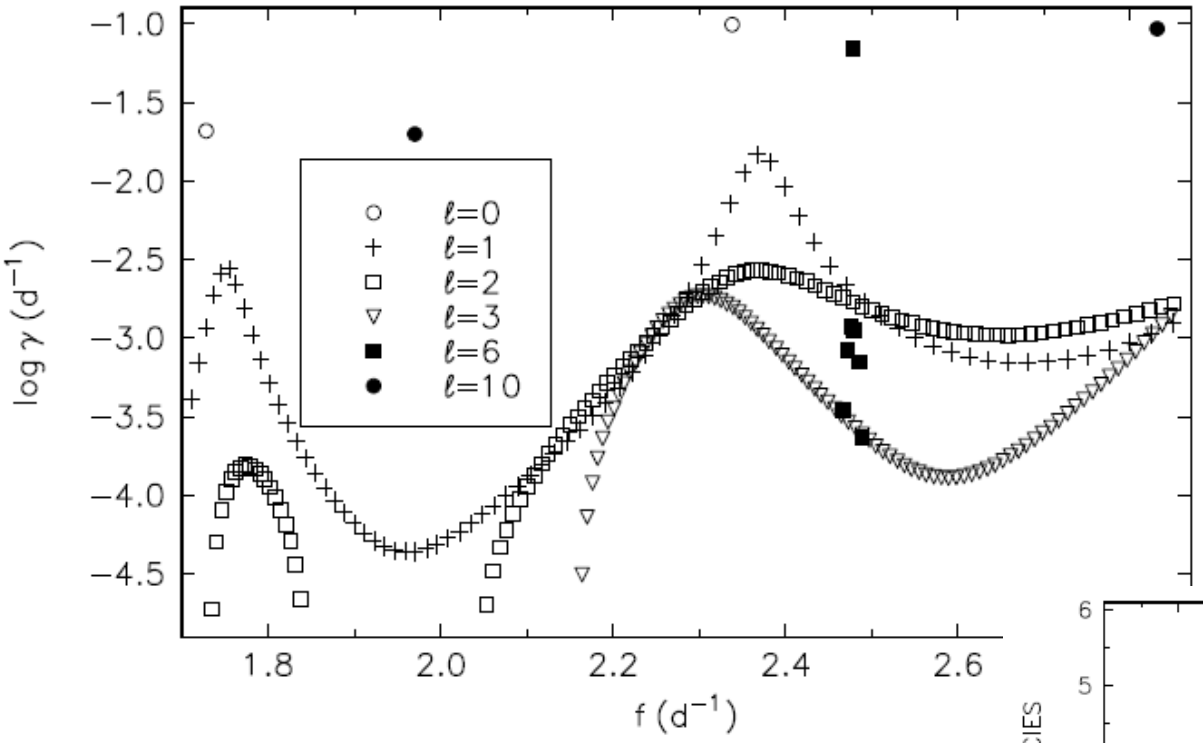

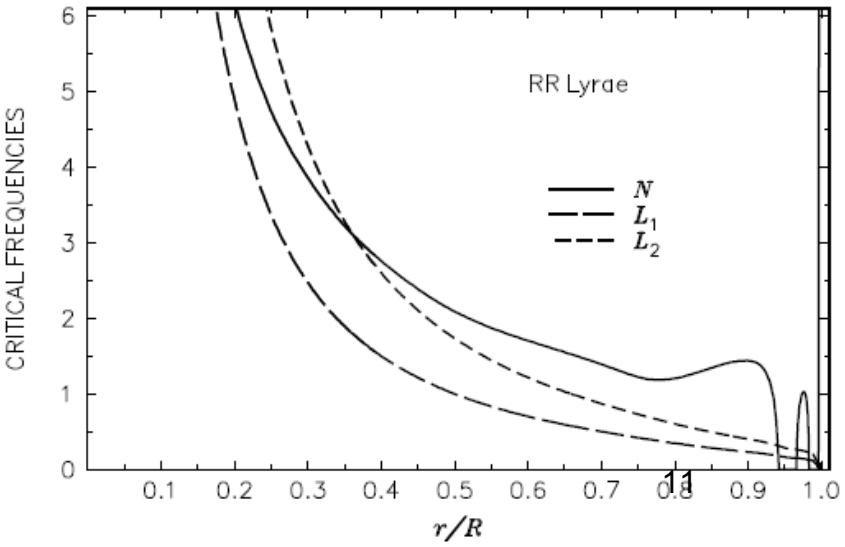

Note:

1. Best trapped **l=1** modes close to l=0
2. Poor trapping of **l=2** and **l=3** modes.

Cepheid models $n_g \sim 10^3\sqrt{\ell}$

no unstable low degree modes

Problems:

1. Applicability of the running wave boundary condition

2. Validity of the Cowling approximation

Avoiding the Cowling approximation

Fourh order system for the four radial eigenfunctions

$$\boldsymbol{\xi} = r[y_1(r)\boldsymbol{e}_r + y_2(r)\boldsymbol{\nabla}_H]Y_\ell^m \mathrm{e}^{-\mathrm{i}\omega}$$

$$\boldsymbol{\nabla}\Phi' = g[y_4(r)\boldsymbol{e}_r + y_3(r)\boldsymbol{\nabla}_H]Y_\ell^m \mathrm{e}^{-\mathrm{i}\omega t}$$

Reduction to second order systems

Asymptotic decomposition in the $A/B \to \infty$ limit

Dz. 1971

$$V_g = \frac{gr}{c^2}$$

$$A = -\frac{d\ln\rho}{d\ln r} - V_g$$

$$U = \frac{4\pi\rho r^3}{M_r}$$

$$B = \frac{\omega^2 r}{g}$$

$$\frac{N}{\omega} = \sqrt{\frac{A}{B}}$$

$$\frac{\mathcal{L}_\ell}{\omega} = \sqrt{\frac{\ell(\ell+1)}{BV_g}}$$

Exact equations for dipolar modes (Takata 2005)

$$(B-1)y_4 + (U-B-2)y_3 + UB(y_1 - y_2) = 0$$

$$V_g = \frac{gr}{c^2}$$

$$\boldsymbol{\xi} = r[y_1(r)\boldsymbol{e}_r + y_2(r)\boldsymbol{\nabla}_H]Y_\ell^m \mathrm{e}^{-\mathrm{i}\omega}$$

$$A = -\frac{d\ln\rho}{d\ln r} - V_g$$

$$\boldsymbol{\nabla}\Phi' = g[y_4(r)\boldsymbol{e}_r + y_3(r)\boldsymbol{\nabla}_H]Y_\ell^m \mathrm{e}^{-\mathrm{i}\omega t}$$

$$U = \frac{4\pi\rho r^3}{M_r}$$

$$z_1 = y_1 + \frac{y_3}{1-B} \qquad z_2 = y_2 + \frac{y_3}{1-B}$$

$$B = \frac{\omega^2 r}{g}$$

$$x\frac{d}{dx}\begin{pmatrix} z_1 \\ z_2 \end{pmatrix} = \begin{pmatrix} V_g - 3 + S & \ell(\ell+1) - BV_g - S \\ 1 - A/B + S & A - 2 - S \end{pmatrix}\begin{pmatrix} z_1 \\ z_2 \end{pmatrix}$$

$$\frac{N}{\omega} = \sqrt{\frac{A}{B}}$$

$$r\frac{\mathrm{d}y_3}{\mathrm{d}r} = (1-U)y_3 + y_4$$

uniform shift

Internal gravity wave

$$\frac{\mathcal{L}_\ell}{\omega} = \sqrt{\frac{\ell(\ell+1)}{BV_g}}$$

$$\begin{pmatrix} y_1 \\ y_2 \\ y_3 \\ y_4 \end{pmatrix} = \tilde{C}_s \begin{pmatrix} 1 \\ 1 \\ -1+B \\ 2-U+B \end{pmatrix} + \tilde{C}_r \begin{pmatrix} 2\mathcal{Z}_1 \\ \mathcal{Z}_2 \\ -UB\mathcal{Z}_1 \\ -UB[\mathcal{Z}_2 + (U-4)\mathcal{Z}_1] \end{pmatrix}$$

$$S = \frac{UB}{(1-B)^2}$$

The acoustic envelope modes

reflected wave neglected

$$-\Psi_I(r_b) = \int_0^{\Psi_b} \left(D - \frac{\omega_I}{\omega_R} \right) \mathrm{d}\Psi_\mathrm{R} \gg 1$$

the running wave boundary condition at the convective envelope bottom

small energy loss $\gamma = -\omega_I = \dfrac{\omega_R |\tilde{C}_r|^2 \Im(\mathcal{Z}_1^* \mathcal{Z}_2)_b (\rho r^5)_b}{I_e + I_c}$

$$I_e = \int_{r_b}^{R} (|y_1|^2 + 2|y_2|^2) \rho r^4 \mathrm{dr}$$

$$I_c = \int_0^{r_b} (|y_{s,1}|^2 + 2|y_{s,2}|^2 \rho r^4 \mathrm{dr} = 3 \left(\frac{\rho \mathrm{r}^5}{\mathrm{U}} \right)_\mathrm{b} |\tilde{\mathrm{C}}_\mathrm{s}|^2$$

The acoustic propagation zone, where modes are trapped

$(\omega - N)(\omega - \mathcal{L}_\ell) < 0$ is not the sufficient no-propagation condition.

There is no such a general condition.

Dipolar modes

approximate condition for the propagation zone bottom: .

$$\omega = \max[\omega_{\rm ac}(r), \mathcal{L}_{1m}(r)]$$

$\omega_{\rm ac}(r)$ local acousic cut-off frequency

$\mathcal{L}_{1m} = \mathcal{L}_1 \left(1 - \frac{U}{3}\right)$ modified Lamb frequency (Takata 2006)

Frequencies of dipolar modes relative radial modes depend on which of The two critical frequencies is first reached.

The acoustic envelope modes

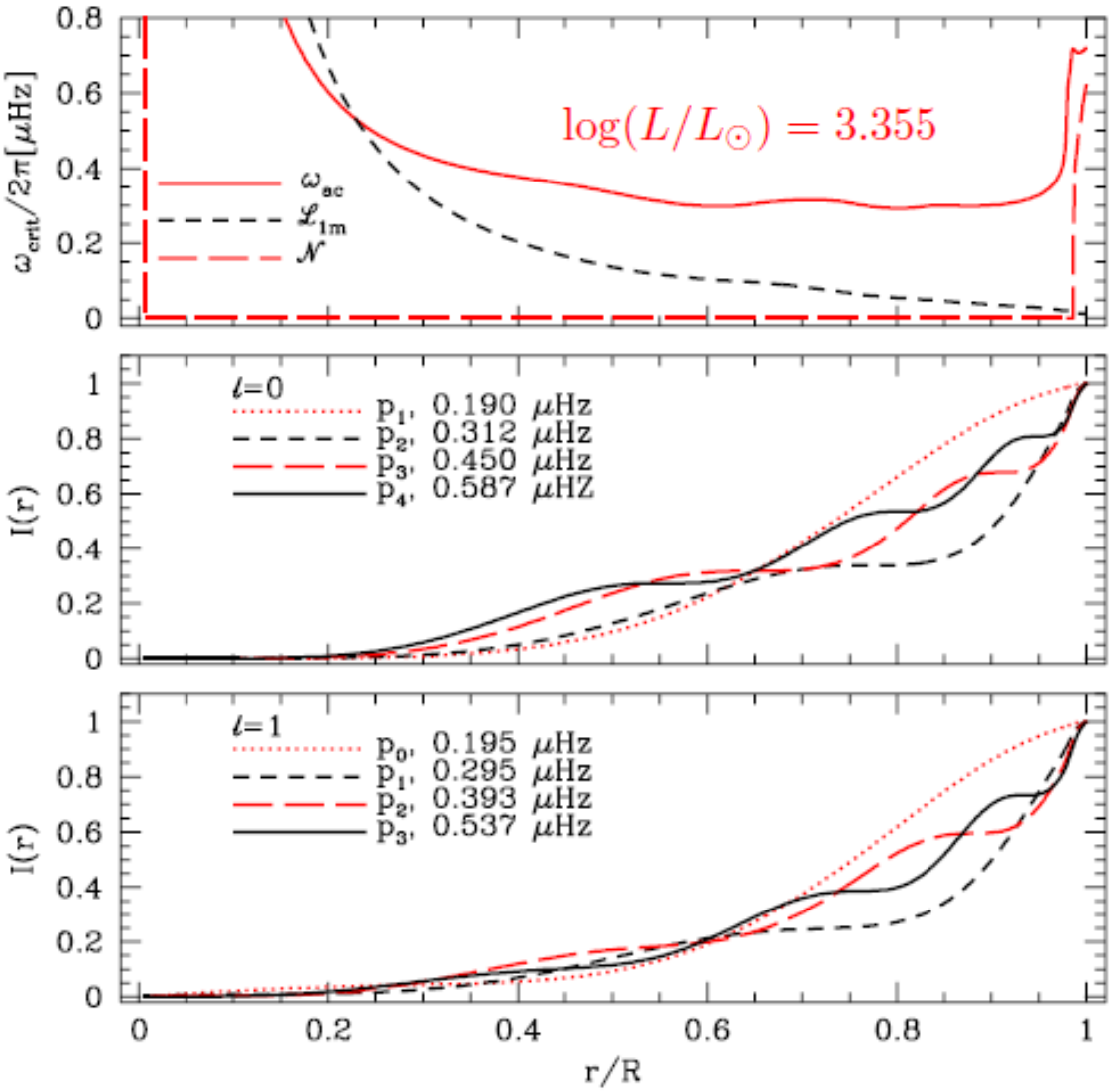

From mixed global modes to envelope acoustic modes

radial and dipolar modes near ν_{max}

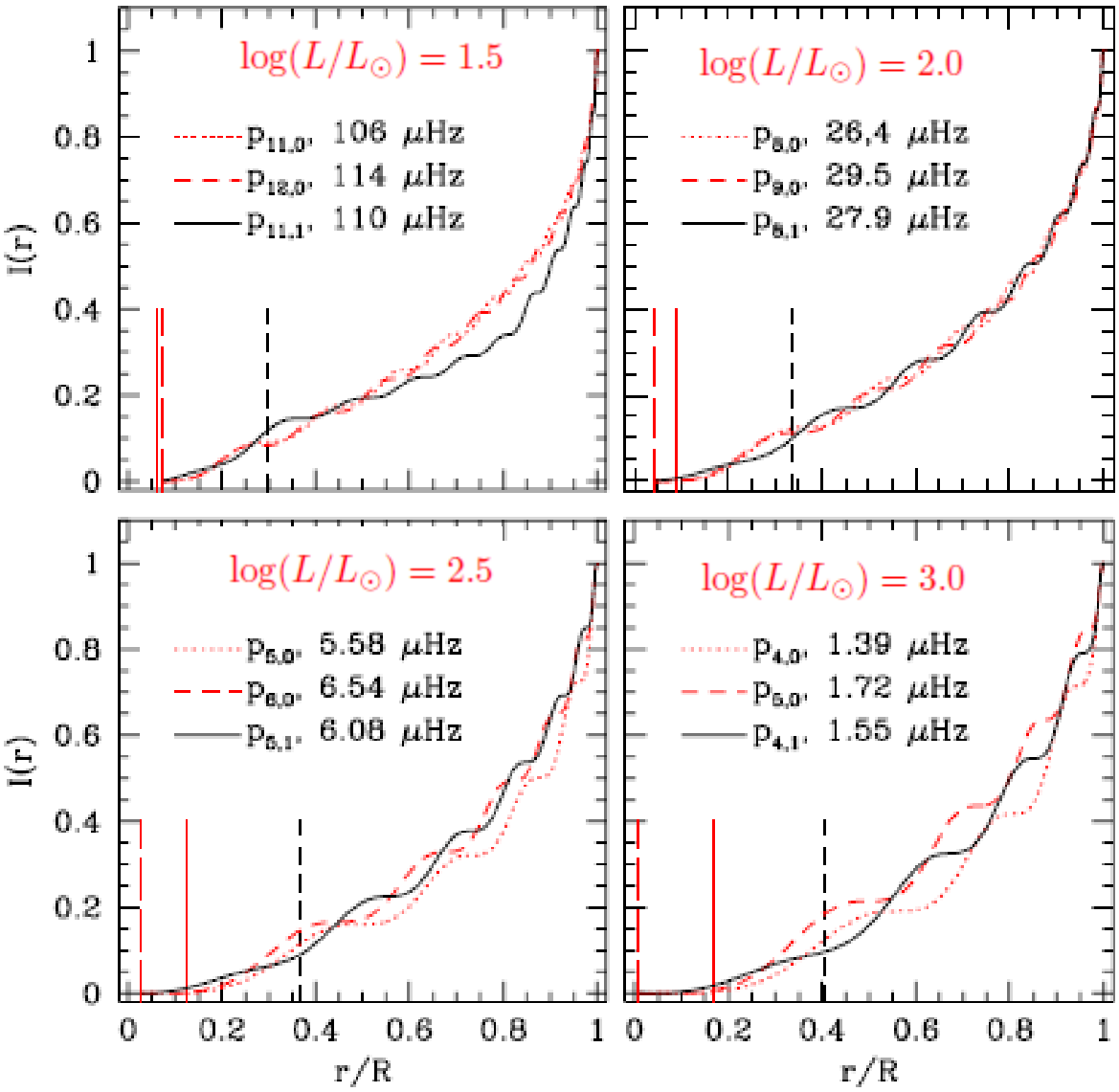

Modes near ν_{max} trapped in convective envelope

$$\delta_n = \frac{0.5(\nu_{n+1,0} + \nu_{n,0}) - \nu_{n,1}}{\nu_{n+1,0} - \nu_{n,0}}$$

damping solely due to wave emission

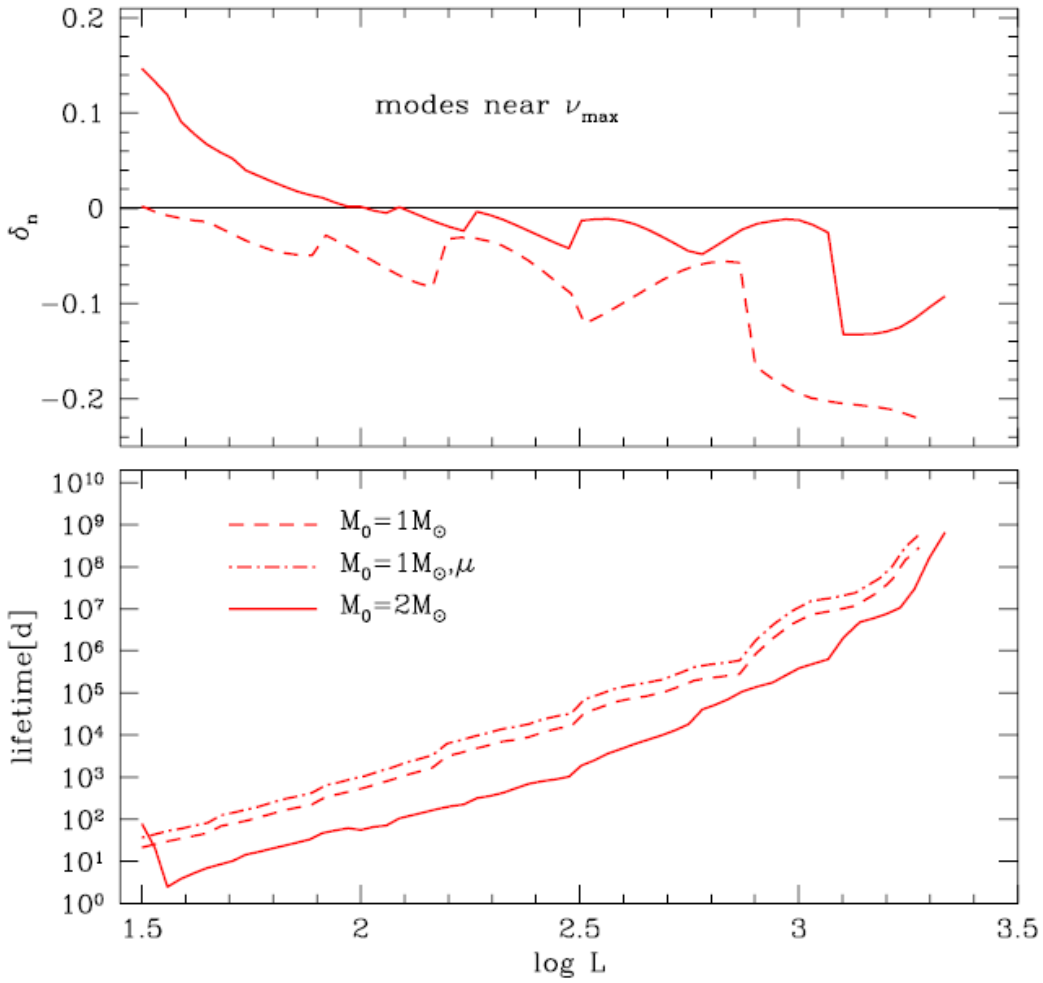

Small in gomparison with damping in outer layers (Dupret et al. 2009) at *L/M*.>100.

CONLUSION

In luminous red giant
the envelope dipolar modes and the radial modes
have very similar properties and
are expected to have similar amplitudes